Nanotechnology **20** (2009) 215301 (9pp) doi:10.1088/0957-4484/20/21/215301

A versatile atomic force microscope for three-dimensional nanomanipulation and nanoassembly

Hui Xie, Dogan Sinan Haliyo and Stéphane Régnier

Institut des Systèmes Intelligents et de Robotique, Université Pierre et Marie Curie/CNRS UMR7222, BC 173, 4 Place Jussieu, F-75005 Paris, France

E-mail: xie@robot.jussieu.fr

Received 9 January 2009, in final form 13 March 2009
Published 5 May 2009
Online at stacks.iop.org/Nano/20/215301

Abstract

A conventional atomic force microscope (AFM) has been successfully applied to manipulating nanoparticles (zero-dimensional), nanowires (one-dimensional) or nanotubes (one- or two-dimensional) by widely used pushing or pulling operations on a single surface. However, pick-and-place nanomanipulation in air is still a challenge. In this research, a modified AFM, called a three-dimensional (3D) manipulation force microscope (3DMFM), was developed to realize 3D nanomanipulation in air. This system consists of two individually actuated cantilevers with protruding tips that are facing each other, constructing a nanotweezer for the pick-and-place nanomanipulation. Before manipulation, one of the cantilevers is employed to position nano-objects and locate the tip of the other cantilever by image scanning. During the manipulation, these two cantilevers work collaboratively as a nanotweezer to grasp, transport and place the nano-objects with real-time force sensing. The manipulation capabilities of the nanotweezer were demonstrated by grabbing and manipulating silicon nanowires to build 3D nanowire crosses. 3D nanomanipulation and nanoassembly performed in air could become feasible through this newly developed 3DMFM.

(Some figures in this article are in colour only in the electronic version)

1. Introduction

Pick-and-place nanomanipulation is a promising technique in 3D nanostructure fabrication since it is an indispensable step in the bottom-up building process. It can overcome limitations of bottom-up and top-down methods of nanomanufacturing and further combine the advantages of these two methods to build complex 3D nanostructures. In the literature, nanostructures have been manipulated, assembled and characterized by integrating nanomanipulators or nanogrippers into scanning electron microscopes (SEM) and transmission electron microscopes (TEM) [1–5]. Both the SEM and the TEM provide a vacuum environment where the van der Waals force is the main force to be overcome during the manipulation. 3D nanomanipulation could also be achieved with optical tweezers in liquid, where the adhesion forces are greatly reduced [6–8]. However, pick-and-place nanomanipulation in air is still a great challenge due to the presence of strong adhesion forces, including van der Waals, electrostatic and capillary forces [9]. In this case, the main difficulties in achieving 3D nanomanipulation are fabricating sharp end-effectors with enough grasping force, as well as the capabilities of force sensing while controlling interactions between the nano-object and the tool or the substrate.

Compared with the nanomanipulation carried out in SEMs and TEMs, the AFM-based nanomanipulation has much more flexibility. It can be applied to various nano-objects in different environments (air, liquid and vacuum). However, the conventional AFM-based nanomanipulation is restricted to pushing and pulling nano-objects on a single surface [10–14]. The pick-and-place manipulation of nano-objects in air is still unresolved using AFMs, although vertical pickup of atoms has been accomplished by electric field trapping [15], van der Waals forces [16, 17], tunneling current-induced heating or by inelastic tunneling vibration [17]. Grasping submicron objects using a two-tip carbon nanotube (CNT) nanotweezer

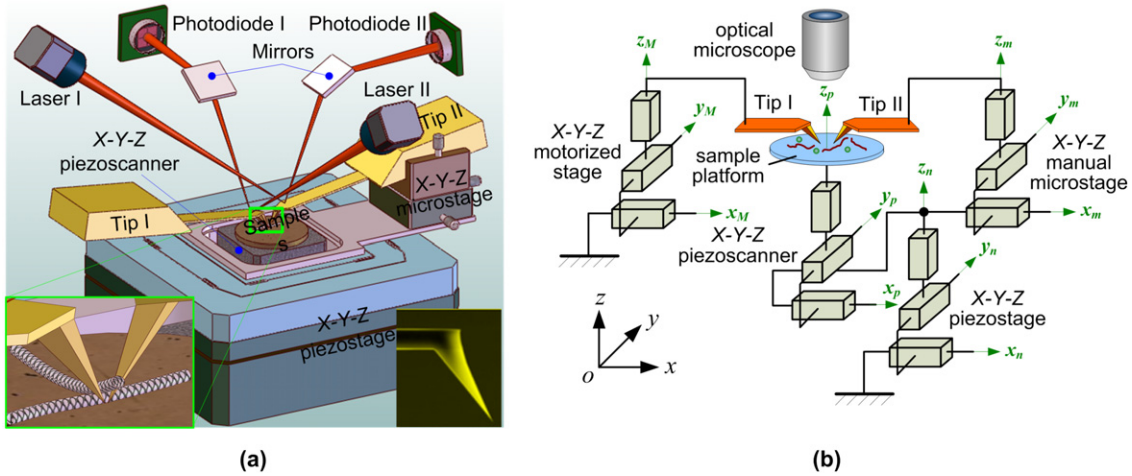

Figure 1. Schematic structure of the 3DMFM. (a) System configuration of the 3DMFM, which consists of two sets of devices commonly used in the conventional AFM. A nanotweezer (left inset) is constructed from two protruding tips of two cantilevers (right inset). (b) Mechanism illustration of the 3DMFM.

has been demonstrated [18], but the alignment between the CNT arms remains a challenge and capabilities of the nanotube nanotweezer in overcoming large adhesion forces in air need further validation. Thus, a versatile 3D nanomanipulation system is crucial in achieving the pick-and-place manipulation in air to build complex 3D nanostructures.

In this paper, we present a two-tip AFM-based nanomanipulation system that is called a 3D manipulation force microscope (3DMFM). This system can be used as a conventional AFM to image, push and pull nano-objects. More importantly, it can achieve pick-and-place nanomanipulation with sufficient force sensing. Two collaborative cantilevers with protruding tips are used in the 3DMFM to construct a two-tip nanotweezer, which can be used to achieve a procedure of 3D nanomanipulation with operations of contact detection, grasping, picking up, transporting and releasing.

We have used the developed 3DMFM to fabricate nanowire crosses by manipulating two types of cone-shaped silicon nanowires (SiNWs). During manipulation, interactive forces applied on the tips were recorded and analyzed. Compared with the means of pick-and-place nanomanipulation realized in the SEM and the TEM, the 3D manipulation process using the developed 3DMFM is more controllable due to the real-time interactive force sensing and the process monitoring, and with much more flexibility in various manipulation environments.

2. System configuration

Figure 1(a) shows the configuration of the 3DMFM, which is equipped with two sets of devices commonly used in conventional AFMs, including cantilevers, optical levers and nanopositioning devices. Two individually actuated cantilevers (ATEC–FM) with protruding tips (as per the right inset of figure 1(a)), namely, Tip I and Tip II, are used as end-effectors to build a nanotweezer (as per the left inset of figure 1(a)). Forces on each cantilever are independently detected by its own optical lever, which is typically composed of a laser and a quadrant photodiode [19]. An X–Y–Z piezostage (MCL Nano-Bio2M on X and Y axes, PI P-732.ZC on Z axis) is used for image scanning and Tip II actuation. The piezostage has a maximum scanning range of 50 μm $\times$ 50 μm $\times$ 10 μm and closed-loop resolutions of 0.1 nm on the X and Y axes, and 0.5 nm on the Z axis with currently used drivers. The other nanopositioning device, an X–Y–Z piezoscanner (PI P–153.10H), is used to transport samples during the manipulation. The piezoscanner has a scanning range of 10 μm $\times$ 10 μm $\times$ 10 μm and a nominal picometer resolution on each axis. Figure 1(b) shows an illustration of a mechanism for a 3DMFM, which can be described in detail as follows.

(1) Tip I, utilized as an imaging tip before manipulation and then as a manipulating end-effector, is fixed on a motorized X–Y–Z stage (not shown in figure 1(a)) for coarse positioning. On the other hand, Tip II, used as a manipulating end-effector supported by a compact manual X–Y–Z microstage for coarse positioning, is mounted on the X–Y–Z piezostage.
(2) The X–Y–Z piezoscanner is fixed on the X–Y–Z piezostage to support and transport samples. Hysteresis and creep of the piezoscanner are accurately characterized and compensated by the Prandtl–Ishlinskii (PI) operator [20] and the logarithmic model [21], respectively.
(3) An optical microscope (Olympus BX50WI) is used to focus and adjust the laser spots on the cantilevers, locate the tips and select interested areas for nanomanipulation.

3. Manipulation protocol

3.1. Overview

As discussed above, the nanotweezer consisting of two protruding tips is used to achieve pick-and-place of nano-objects deposited on the substrate due to its very sharp tip ends with a radius less than 10 nm and the capability of real-time force sensing. Once the tips and the nano-objects are

accurately located using image scanning, the nanotweezer is formed to pick up and transport the selected nano-objects to the target positions. The details of manipulation schemes and a protocol of the 3DMFM are discussed in the following.

3.2. Pick-and-place protocol

Nanowires and nanotubes are being intensively investigated as promising nanomaterials for application to nano-optics, nanoelectronics and nanoelectromechanical systems (NEMS). Thus, a protocol of the 3DMFM is presented specifically for application to nanowires or nanotubes deposited on a substrate. Applications of such a protocol can easily be extended to the pick-and-place of nanoparticles dispersed on a substrate. Figure 2(a) shows a procedure for the pick-and-place nanowire manipulation, which involves the following steps.

3.2.1. System initialization. Once the manipulation area is selected, both the tips are aligned as a quasinanotweezer above the center of the manipulation area under the optical microscope. Each axis of the piezostage and the piezoscanner is initialized on a proper position. The initialization should provide enough motion range for the nanomanipulation within an image scanning area.

3.2.2. Image scanning. This step is started from locating Tip II by locally scanning its end with Tip I. The image scanning length on Tip II is determined by its image height, which should have the roughly equal maximum image height as the nano-objects. Once the local scanning on Tip II is completed, Tip I is used to fully scan the interested region, obtaining a topographic image that contains the nano-objects to be manipulated and, of course, the Tip II end. This step is depicted in figure 2(a)-I, in which the piezostage is actuated for the image scan from left to right on the X axis. Figure 2(b) shows a simulated image that contains the topography of the two nanowires and the end of Tip II.

3.2.3. Relocating Tip II. After a long image scanning, relocating Tip II is quite necessary to succeed in constructing the nanotweezer due to the system's thermal drift, which will cause noticeable positioning errors if the nanomanipulation is performed in an uncontrolled environment. The relocation of Tip II is performed by the same local scanning operation as described in section 3.2.2.

3.2.4. Making Tip II–nanowire in contact. Figure 2(a)-II shows that Tip II approaches the nanowire to make a contact by moving the X axis of the piezoscanner. A gap (typically 5–20 nm above the snap-in bound) between Tip II and the substrate should be kept during the approach because it enables a negative deflection response as a tiny force applied on Tip II, hence, a sensitive detection of the tip–nanowire contact.

3.2.5. Constructing the nanotweezer. Similarly, as the step depicted in figure 2(a)-III, Tip I approaches the nanowire by moving the X axis of the piezostage. Once the Tip I and the nanowire are in contact, a nanotip nanotweezer is configured for a grasping operation of the nanowire.

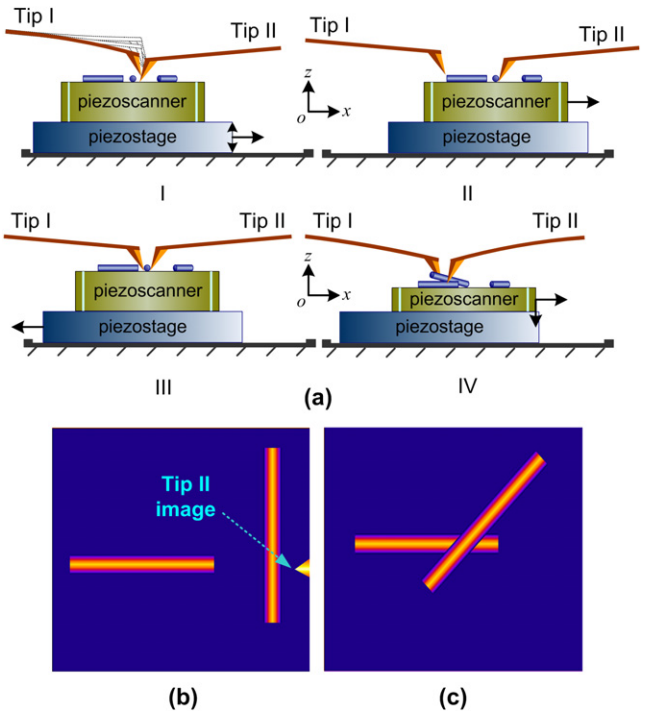

Figure 2. Protocol of the pick-and-place of nanowires for building a nanowire cross. (a) Four main steps involved in a pick-and-place procedure. Image scanning in step I; Tip II approaches nanowire by moving the X axis of the piezoscanner in step II; in step III Tip I approaches the grasping location on the same nanowire to construct a nanotweezer by moving the X axis of the piezostage; the pick-and-place manipulation is achieved in step IV. (b) Simulated image before the manipulation, by which locations of nanowires and Tip II are recorded. (c) Simulated image of a nanocross is built by the pick-and-place nanomanipulation.

3.2.6. Pick-and-place. In this step, as shown in figure 2(a)-IV, the nanotweezer is used to pick up, transport and place the nanowire to its target position by moving the piezoscanner on the X, the Y or the Z axis. The displacement on each axis depends on the dimensions of the nanowire and the location of its destination.

3.2.7. Re-initialization. Initialize the piezoscanner and the piezostage. Then the manipulation procedure is repeated for the next nanowire.

3.3. Force sensing during pickup

Figure 3 shows a force simulation during the nano-object pickup operation with the nanotweezer. Interactive forces applied on the nanotweezer include repulsive forces, friction forces and adhesive forces. The interactive forces on the nanotweezer can be resolved into two components on the X axis and the Z axis in the defined frame, for example on Tip I, namely F_{x1} and F_{z1}, respectively. The component force on the X axis is the clamping force that holds the nano-object. On the other hand, the component force on the Z axis is the pickup force that balances the adhesion forces from the substrate. In order to measure the interactive forces, further analysis is

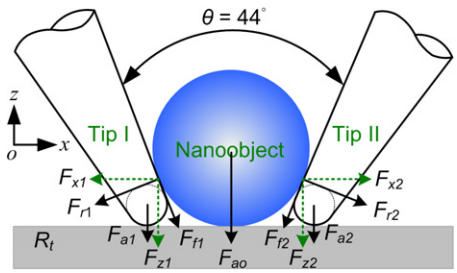

Figure 3. Force simulation of pickup manipulation with a nanotweezer constructed from two cantilever tips. The nanotweezer has a clamping angle of 44°.

carried out to estimate these two component forces, both of which result in bending deformation of the cantilevers.

Taking Tip I for instance, F_{x1} and F_{z1} can be calculated in the defined frame by

$$F_{z1} = F_{r1}\left(\mu\cos\frac{\theta}{2} + \sin\frac{\theta}{2}\right) + F_{a1} \tag{1}$$

$$F_{x1} = F_{r1}\left(\cos\frac{\theta}{2} - \mu\sin\frac{\theta}{2}\right) \tag{2}$$

where F_{r1} is the repulsive force, $\mu F_{r1} = F_{f1}$ is the friction force, μ is the friction coefficient, θ is the clamping angle of the nanotweezer and F_{a1} is the adhesive force between Tip I and the substrate.

For convenience of calculation, the angular deflection of the cantilever is adopted due to its linear relation with the voltage output of the optical lever. The bending angular deflection on the free end of the cantilever comprises two parts: ϕ_{z1} and ϕ_{x1}, which are caused by F_{z1} and F_{x1}, respectively. These two parts can be calculated by

$$\phi_{z1} = \frac{F_{z1}L^2}{2EI} \tag{3}$$

$$\phi_{x1} = \frac{F_{x1}Ll}{EI} \tag{4}$$

where L is the effective length of the cantilever, l is the cantilever's tip height, E is Young's modulus of the silicon and I is the moment of inertia on the cantilever's cross section. L and l are measured as 250 μm and 9.5 μm, respectively.

Here we set $\mu = 0.33$, which is one of the experimental values obtained from an AFM lateral force calibration using a silicon grating [22]. As seen in figure 3, the nanotweezer has a clamping angle $\theta = 44°$. Thus, without consideration of F_{a1}, from equations (1)–(4), a simplified relation between ϕ_{z1} and ϕ_{x1} can be estimated as

$$\phi_{x1} \approx 0.089\phi_{z1}. \tag{5}$$

Actually, the magnitude of the adhesion force F_{a1} is often comparable to that of the repulsive force F_{r1} until the nanotweezer pulls off the substrate. In this case, the angular deflection produced by F_{x1} will be approximately reduced to less than half of the estimate from equation (5). Therefore, for simplifying the estimating process of the adhesion forces F_{ao}, the cantilever deflection caused by F_{x1} will be neglected in the following calculations. Thus, the F_{z1} can be easily estimated from the normal voltage output of the optical lever of Tip I by [23]

$$F_{z1} = \beta_1\Delta V_1 \tag{6}$$

where β_1 and ΔV_1 are the calibrated normal force sensitivity [24] and voltage output of the optical lever of Tip I, respectively. A similar result can be obtained from Tip II. Once the F_{z1} and F_{z2} are known, for equilibrium, the adhesion force F_{ao} applied to the nano-object can be estimated as

$$F_{ao} = F_{z1} + F_{z2} = \beta_1\Delta V_1 + \beta_2\Delta V_2 \tag{7}$$

where β_2 and ΔV_2 are the normal force sensitivity and voltage output of the optical lever of Tip II, respectively.

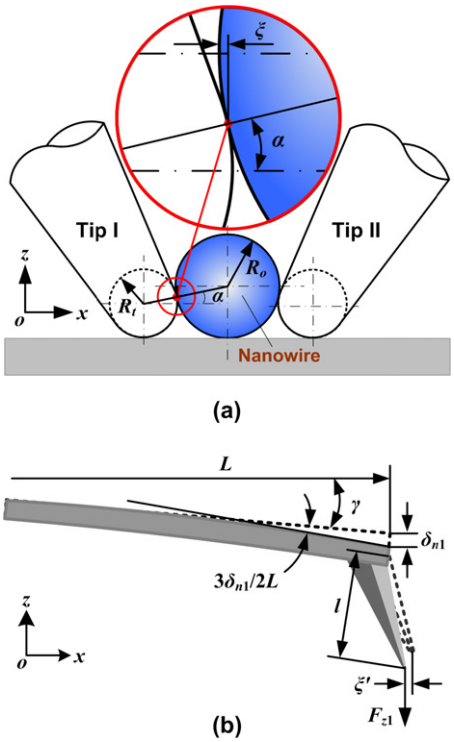

Figure 4. Schematic for manipulation limit calculation. (a) In order to complete the grasping operation, the angle α and the dig-in distance ξ should be positive. The top inset shows details confined in the red circle. (b) Illustration for ξ' calculation.

3.4. Grasping limit of the nanotip tweezer

However, every manipulation system has its own limitations on the size of the objects to be manipulated. In the proposed 3DMFM, the minimum size of the nano-object that can be manipulated is limited by the tip size. For nanowire grasping, the nanoscale nanotweezer–nanowire contact area leads to a weak contact friction that is proportional to the contact area at nanoscale [25]. These friction forces in general are not strong enough to overcome the large adhesion forces of the nanowire–substrate contact. Fortunately, for the proposed nanotip tweezer, as seen in figure 4(a), a positive clamping angle is adopted that makes grasping stronger due to repulsive

forces from the tip–nanowire contact which combines with the tip–nanowire friction forces to overcome the strong adhesion forces from the contact with the substrate.

On the assumption that no preload is applied to the nanowire before the pickup operation, as shown in figure 4(a), in order to complete the grasping, the angle α and the dig-in distance ξ should be positive, which can be calculated via a simple geometric transform:

$$\alpha = \arcsin\left(\frac{R_o - R_t}{R_o + R_t}\right) \tag{8}$$

$$\xi = R_o(1 - \cos\alpha) \tag{9}$$

where R_o and R_t are the radii of the nanowire and the tip, respectively.

During the pickup operation, the tip end will retract a small distance ξ' because of the deflection on the cantilever beam. This retraction will reduce the effective dig-in distance. Figure 4(b) shows an illustration to calculate the retracting distance ξ' taking no account of the tip deformation based on the fact that the tip stiffness is typically two to three orders of magnitude larger than the normal stiffness of the cantilever [26]. Therefore, with a very small deflection $\delta_{n1} = F_{z1}/k_1$ on the free end of the cantilever beam, ξ' can be estimated as

$$\xi' = -\frac{F_{z1}}{k_1}\left(\frac{3l}{2L}\cos\gamma + \tan\gamma\right) \tag{10}$$

where k_1 is the bending stiffness of the cantilever, γ is the cantilever's mounting angle, L is the effective length of the cantilever and l is the tip height. Here, deflection caused by the force F_{x1} is neglected as discussed in section 3.3. Therefore, in order to achieve the grasping operation with the nanotweezer, the effective dig-in distance should satisfy

$$\xi + \xi' > 0. \tag{11}$$

Thus, from equation (11), the minimum diameter of the nanowire R_{min} can be calculated by

$$R_{min}\left(1 - \sqrt{1 - \frac{(R_{min} - R_t)^2}{(R_{min} + R_t)^2}}\right) = \frac{F_{z1}}{k_1}\left(\frac{3l}{2L}\cos\gamma + \tan\gamma\right). \tag{12}$$

For example, during the pickup, if the maximum $F_{z1} = 50$ nN, $R_t = 8$ nm, $k_1 = 4$ N m^{-1}, $\gamma = 5°$, $L = 250$ μm and $l = 10$ μm, the minimum diameter of the nano-objects that can be picked up is $D_{min} = 2R_{min} = 39.4$ nm. If a worn tip with $R_t = 15$ nm is used, the minimum diameter of the nano-objects will increase to $D_{min} = 61.1$ nm.

It should be clear that this limit is calculated on the assumption that no grasping force exists prior to the pickup operation. If the nanotweezer holds the nanowire more tightly, leading to a smaller gap between the two tips before pickup, the minimum diameter that can be manipulated should be reduced a lot. However, the preload involves great risks in damaging the tips as well as the nano-objects.

In addition, sharper AFM tips extended with single-walled carbon nanotubes (SWNT) or multi-walled carbon nanotubes (MWNT) may bring the 3DMFM a promising breakthrough in the grasping limit [27]. Another possibility is to manipulate suspended nano-objects, because in this case more space will be provided to obtain a closer grasping gap between the tweezer tips, bypassing the restriction from the dig-in distance.

4. Pick-and-place nanomanipulation

4.1. Sample preparation

Uniformly well-dispersed deposition of the nanoparticles or nanowires usually cannot be achieved by simply drying a colloid drop on a substrate. In our experiments, SiNW arrays were grown on Si wafers using chemical vapor deposition (CVD). In sample preparation, a freshly cleaned silicon wafer coated with 300 nm silicon dioxide was placed in parallel with the sample surface of SiNWs. Then the SiNW array is lightly scratched and SiNWs were uniformly attached to the silicon substrate due to the adhesive forces. AFM images show that the SiNWs have a taper shape. In pick-and-place experiments, two types of cone-shaped SiNWs diameters were manipulated to build nanowire crosses. One type of SiNWs has a diameter of 15 (top)–70 nm (root) and a length of 3–4 μm. The other SiNWs have diameters of 25 (top)–200 nm (root) and lengths of about 7 μm.

4.2. Contact detection

In general, manipulating an object requires the ability to observe, position and physically transport the object. Unlike the nanomanipulation performed in the SEM or the TEM, the AFM manipulation has no real-time vision feedback to monitor the manipulation process. In this case, real-time force feedback is necessary to detect the interaction between the tips and the nano-objects. In the 3DMFM pick-and-place manipulation, contact detection is a significant step for a successful grasping of the nano-objects. In order to detect the interaction between the nano-object and the tip in the grasping operation, a tiny gap between the tip and the substrate (typically 5–20 nm) should be kept when the tip approaches the nano-object. In the grasping operation, as the tip approach and further 'digs into' the base of the nano-object after contact, this gap enables the cantilever's bending deformation and hence precise normal force sensing.

Figure 5 shows an example of the contact detection with Tip II, which is obtained by grabbing an SiNW with a diameter of 25 (top)–200 nm (root) and a length of 7 μm. The grasping location is near the root of the nanowire. The curve starts from the noncontact state with neither substrate nor the nanowire. As the tip further moves towards the nanowire, the cantilever is bent upward (about 3 nm) leading to positive forces after position 'A' marked in figure 5. Two factors could contribute to this positive response: chemical dirt on the border of the nanowire and adhesion forces from the nanowire.

The tip starts to dig into the base of the nanowire as its positive response reaches the first peak of 7.4 nN and then contacts the nanowire. In this part, before the tip contacts the substrate, the bending force decreases rapidly to −12 nN

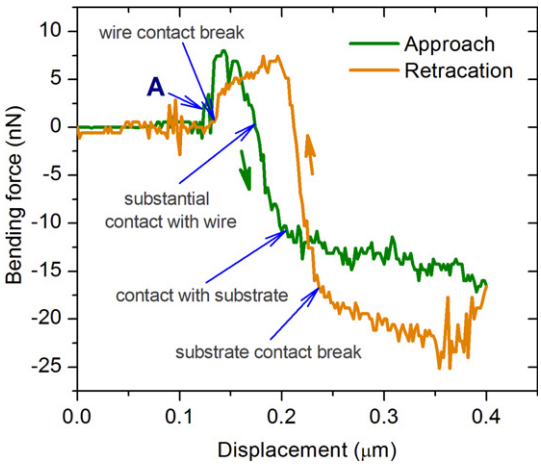

Figure 5. Contact detection by the normal force sensing on Tip II. The force curve shows the bending behavior of the cantilever during the steps of approach, contact and retraction.

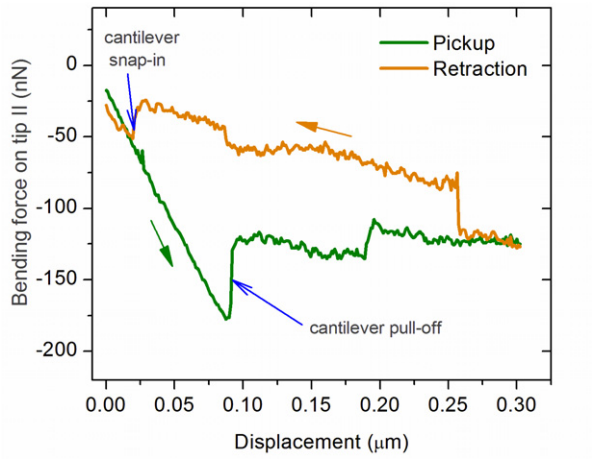

Figure 6. Force detection on Tip II during the pickup operation. The force curve shows the bending behavior of the cantilever during the processes of pickup and retraction for releasing.

with a short displacement of about 35 nm. The further move leads to the pushing of the nanowire, causing a slow decrease of the bending force due to the tip deformation. During the retraction, the adhesion forces between the tip and the substrate induces a sudden decrease of the bending force to −24 nN. After the contact breaks with the substrate, the bending force sharply reaches a positive peak with a similar value than the former peak in the approach path. Eventually, the tip returns to position 'A' with the same force response and reaches zero. This confirms that the positive peaks around the contact point in the approach and retraction paths are due to the contribution of the unmoved chemical dirt.

The force response described in figure 5 is sufficient to detect not only the contact between the tip and the nano-object, but the grasping state. In our experiments, as contact between Tip II and the nanowire is detected, Tip II retracts a little with a displacement of 5–20 nm in order to keep a tiny gap between Tip II and the substrate, enabling the confirmation of grasping state as Tip I contact the nanowire.

4.3. Force sensing in the pick-and-place task

Figure 6 shows a curve of the peeling force spectroscopy on Tip II for the pick-and-place manipulation of the same nanowire on the same manipulating location used in the contact detection experiment. The curve starts from the contact state among the nanotweezer, the nanowire and the substrate. As the piezoscanner is moved down to pick up the nanowire, the cantilever is bent, leading to negative forces. During the pickup, when the position reaches 88 nm, the cantilever pulls off the substrate with a pull-off force of 52 nN, and the force returns to −125 nN. As the piezoscanner is moved down further, the force magnitude keeps slightly decreasing to a value of −136 nN at 188 nm. After this point, the magnitude of the force suddenly falls to −110 nN, forming a tiny force peak of 5 nN. Further pickup leads to another slow decrease of the peeling force to −125 nN at 302 nm. At the first part of the retraction, as the tips approach the substrate, the force slightly increases from −126 to −118 nN at 258 nm. A sudden increase of 43 nN occurs at this point with a further retraction. Further retraction leads to a continuous increase except for a weak fluctuation between 135 and 81 nm. Snap-in occurs at 21 nm after a mild decrease of the force. The snap-in force reaches −21 nN. Upon still further retraction, the magnitude of the normal force of Tip II approaches the previous grasping state.

The force responses on Tip I are similar in the shape of curve except for the force magnitude due to different force sensitivities on each tip and an uneven grasping due to asymmetric alignment of the nanowire related to the grasping direction.

Such a force spectroscopy curve during the pickup operation shows a stable grasping for further transport. A full force response of the nanowire pick-and-place is not shown here, but a simple description is shown in figure 7(d).

4.4. Manipulation results

In order to validate the pick-and-place manipulation abilities of the developed 3DMFM, two types of cone-shaped SiNWs were manipulated and two nanocrosses were achieved. Figure 7 shows the manipulation processes and result with SiNWs with diameters of 25 (top)–200 nm (root). A pre-scanned image (9 μm × 9 μm) is shown in figure 7(a), which includes the topographic image of several nanowires and, of course, also involves the local image of Tip II (see the inset for its topography enlargement). In figure 7(a), a grasping location of the nanowire to be manipulated is marked with a short green line A–A, where the nanowire has a height of 166 nm, as shown in the top inset. Figure 7(b) shows the re-scanned image after pick-and-place manipulation. It can be seen that the nanowire has been successfully transported and placed onto another nanowire to build a nanocross. A panorama of the nanocross is shown in figure 7(c), by which we can find that the manipulated SiNW has a length of 7.1 μm and its trail before manipulation is clearly marked by the chemical dirt. The nanowire cross has a maximum height about 800 nm, forming a huge 3D nanostructure. A full force curve was recorded

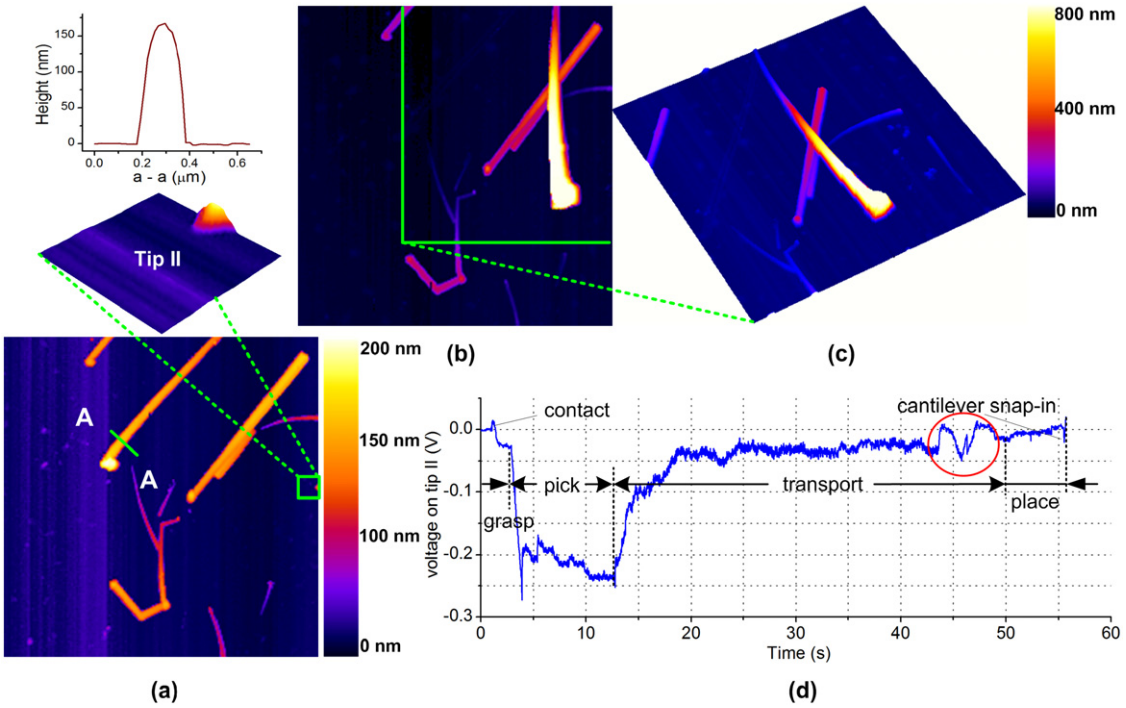

Figure 7. Pick-and-place manipulation results of cone-shaped SiNWs with diameters of 25 (top)–200 nm (root) and with a full length of about 7 μm, in which the image scan size is 9 μm $\times$ 9 μm. (a) An image scanned before the manipulation, which includes the topographic images of the nanowires and location information of Tip II. The top insets show the topography enlargement of Tip II and provide height information at the grasping location A–A. (b) A new scanning image after pick-and-place manipulation verifies that a successful nanocross has been built. (c) Another new scanning image shows a panorama of the nanocross. (d) A full force curve on Tip II recorded during the whole procedure of pick-and-place manipulation.

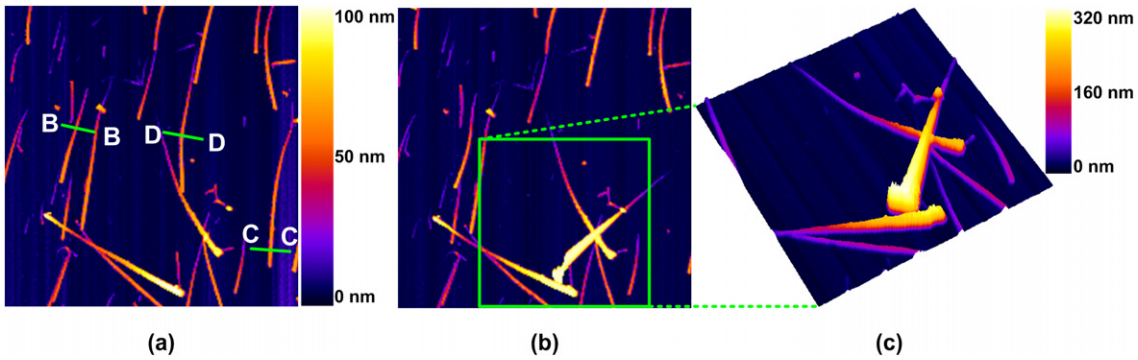

Figure 8. Pick-and-place manipulation results of cone-shaped SiNWs with diameters of 15 (top)–70 nm (root) and with lengths of 3–4 μm. (a) An image scanned of size 8 μm $\times$ 8 μm before the manipulation, in which three nanowires were selected for the manipulation. Corresponding manipulation locations are marked as B–B, C–C and D–D where nanowire heights are 46 nm, 66 nm and 58 nm, respectively. (b) A new image scanned after the manipulation, which shows that the first grasping on location B–B is unsuccessful due to the manipulation limit, the second manipulation on C–C built a perfect nanocross, while the last manipulated nanowire stuck to Tip II due to the improper manipulating location D–D. (c) A topographic enlargement of the nanocross.

from the force response on Tip II, as shown in figure 7(d). The force curve exhibits four main steps in the pick-and-place manipulation, including grasping, picking up, transporting and placing. The manipulation procedure is described as follows.

Once the SiNW was reliably grasped, the piezoscanner moved down 650 nm with a velocity of 65 nm s^{-1} and the photodiode voltage output decreased to 0.24 V before the third step. In this step, the SiNW was transported a distance of 4.6 μm on the X axis with a velocity of 120 nm s^{-1} and 0.18 μm on the Y axis with a smaller velocity of 4.8 nm s^{-1}. During the nanowire transport, a disorder (marked by a red circle) occurred due to its contact with the supporting nanowire before releasing. In the releasing step, the piezoscanner moved up with a velocity of 100 nm s^{-1}. As Tip II was slightly bent upward leading a positive response of 0.015 V, Tip I and Tip II were separated by moving the piezostage on the X axis to open the nanotweezer.

Figure 8 shows the manipulation process and results of the other type of cone-shaped SiNWs with diameters of 15 (top)–70 nm (root). After image scanning, as shown in figure 8(a),

three SiNWs were selected and the manipulation locations were placed near the top, near the root and on the middle part of the nanowires, marked by short green lines B–B, C–C and D–D, where the heights of the SiNWs are 46 nm, 66 nm and 58 nm, respectively. During the first grasping on location B–B, after successful contact detection on Tip II, as Tip I approaches the nanowire to form a nanotweezer, the 'dig-in' response as shown in figure 5 did not happen. Consequently, the first SiNW could not be picked up but be pushed by Tip I, which is verified in figure 8(b). Two factors could contribute to the failure of the grasping: some chemical dirt on the way to 'dig into' and another significant factor is that the worn Tip I after image scanning reached its manipulation limit for pickup. On the second manipulation location C–C, the 3DMFM succeeded in pick-and-place manipulation and building a nanocross, as shown in the image enlargement in figure 8(c). A similar force response during the manipulation was obtained as figure 7(d) shows, with the difference that the magnitude of the force was of the order of several to tens of nanoNewtons. Another failure happened in the manipulation of the third nanowire on its middle part, as marked at location D–D. Force detection indicated the 3DMFM succeeded in grasping, but during the pickup or transportation process, the SiNW jumped from the substrate and stuck to Tip II. This failure was confirmed by abnormal behavior on local scanning with Tip II using the tapping mode.

The last failure in the second manipulation indicates that the sticking problem still exists in the 3DMFM for the nanowire pick-and-place manipulation. To mitigate such failings, the grasping location is highly recommended at the end of the nanowire. Moreover, the nanowire should keep in contact with the substrate during the entire process of pick-and-place.

5. Conclusion

It is well known that the pick-and-place nanomanipulation in air is still a challenge. Fortunately, the 3D manipulation force microscope (3DMFM) presented here has achieved this type of pick-and-place nanomanipulation using a nanotweezer formed by two AFM cantilevers. Each cantilever is equipped with a nanopositioning device and an optical lever, enabling the 3DMFM to have the capabilities of image scanning and real-time force sensing during pick-and-place manipulation. In order to validate the manipulation capabilities of the 3DMFM, two types of cone-shaped SiNWs were manipulated and two nanowire crosses were achieved. Moreover, force recording during the pick-and-place manipulation provides valuable data in the understanding of the nanomechanics and nanophysics. As a result, the 3DMFM makes the 3D nanomanipulation and nanoassembly, such as constructing 3D nanostructures, building 3D nanodevices and revealing nanomechanics phenomena, more practical.

However, the 3DMFM needs to be improved or some remaining problems and uncertainties need to be resolved, such as thermal drift characterization and compensation among the two tips and nano-objects, automated or user-guided nanoparticles' pick-and-place manipulation and tip modifications in relation to the limitations on sizes of the nano-objects to be manipulated.

Acknowledgments

This work has been supported by the French National Agency of Research, through the NANOROL project. The authors would like to thank Dr L W Yu for kindly providing SiNWs for experiments.

References

[1] Fukuda T, Arai F and Dong L X 2003 Assembly of nanodevices with carbon nanotubes through nanorobotic manipulations *Proc. IEEE* **91** 1803–18
[2] Dong L X, Arai F and Fukuda T 2002 Electron-beam-induced deposition with carbon nanotube emitters *Appl. Phys. Lett.* **81** 1919–21
[3] Dong L X, Arai F and Fukuda T 2004 Destructive constructions of nanostructures with carbon nanotubes through nanorobotic manipulation *IEEE/ASME Trans. Mechatronics* **9** 350–7
[4] Molhave K, Wich T, Kortschack A and Boggild P 2006 Pick-and-place nanomanipulation using microfabricated grippers *Nanotechnology* **17** 2434–41
[5] Dong L X, Tao X Y, Zhang L, Nelson B J and Zhang X B 2007 Nanorobotic spot welding: controlled metal deposition with attogram precision from copper-filled carbon nanotubes *Nano Lett.* **7** 58–63
[6] Leach J, Sinclair G, Jordan P, Courtial J, Padgett M J, Cooper J and Laczik Z J 2004 3D manipulation of particles into crystal structures using holographic optical tweezers *Opt. Express* **12** 220–6
[7] Yu T, Cheong F C and Sow C H 2004 The manipulation and assembly of CuO nanorods with line optical tweezers *Nanotechnology* **15** 1732–6
[8] Bosanac L, Aabo T, Bendix P M and Oddershede L B 2008 Efficient optical trapping and visualization of silver nanoparticles *Nano Lett.* **8** 1486–91
[9] Rollot Y, Régnier S and Guinot J C 1999 Simulation of micromanipulations: adhesion forces and specific dynamic models *Int. J. Adhes. Adhes.* **19** 35–48
[10] Falvo M R, Taylor R M I, Helser A, Chi V, Brooks F P J, Washburn S and Superfine R 1999 Nanometre-scale rolling and sliding of carbon nanotubes *Nature* **397** 236–8
[11] Baur C, Bugacov A, Koel B E, Madhukar A, Montoya N, Ramachandran T R, Requicha A A G, Resch R and Will P 1998 Nanoparticle manipulation by mechanical pushing: underlying phenomena and real-time monitoring *Nanotechnology* **9** 360–4
[12] Resch R, Lewis D, Meltzer S, Montoya N, Koel B E, Madhukar A, Requicha A A G and Will P 2000 Manipulation of gold nanoparticles in liquid environments using scanning force microscopy *Ultramicroscopy* **82** 135–9
[13] Sitti M, Horiguchi S and Hashimoto H 2000 Controlled pushing of nanoparticles: modeling and experiments *IEEE/ASME Trans. Mechatronics* **5** 199–211
[14] Yun Y J, Ah C S, Kim S, Yun W S, Park B C and Ha D H 2007 Manipulation of freestanding Au nanogears using an atomic force microscope *Nanotechnology* **18** 505304
[15] Whitman L J, Stroscio J A, Dragoset R A and Cellota R J 1991 Manipulation of adsorbed atoms and creation of new structures on room-temperature surfaces with a scanning tunneling microscope *Science* **251** 1206–10
[16] Eigler D M and Schweizer E K 1990 Positioning single atoms with a scanning tunneling microscope *Nature* **344** 524–6
[17] Avouris P 1995 Manipulation of matter at the atomic and molecular-levels *Acc. Chem. Res.* **28** 95–102
[18] Kim P and Lieber C M 1999 Nanotube nanotweezers *Science* **286** 2148–50

[19] Xie H, Vitard J, Haliyo S and Régnier S 2008 Optical lever calibration in atomic force microscope with a mechanical lever *Rev. Sci. Instrum.* **79** 096101
[20] Krejci P and Kuhnen K 2001 Inverse control of systems with hysteresis and creep *IEE Proc., Control Theory Appl.* **148** 185–92
[21] Jung H and Gweon D 2000 Creep characteristics of piezoelectric actuators *Rev. Sci. Instrum.* **71** 1896
[22] Varenberg M, Etsion I and Halperin G 2003 An improved wedge calibration method for lateral force in atomic force microscopy *Rev. Sci. Instrum.* **74** 3362–7
[23] Xie H, Vitard J, Haliyo S and Régnier S 2008 Enhanced accuracy of force application for AFM nanomanipulation using nonlinear calibration of optical levers *IEEE Sensors J.* **8** 1478–85
[24] Xie H, Vitard J, Haliyo S, Régnier S and Boukallel M 2008 Calibration of lateral force measurements in atomic force microscopy with a piezoresistive force sensor *Rev. Sci. Instrum.* **79** 033708
[25] Carpick R W, Ogletree D F and Salmeron M 1997 Lateral stiffness: a new nanomechanical measurement for the determination of shear strengths with friction force microscopy *Appl. Phys. Lett.* **70** 1548–50
[26] Lantz M A, O'shea S J, Hoole A C F and Welland M E 1997 Lateral stiffness of the tip and tip–sample contact in frictional force microscopy *Appl. Phys. Lett.* **70** 970
[27] Lee H W, Kim S H, Kwaka Y K and Han C S 2005 Nanoscale fabrication of a single multiwalled carbon nanotube attached atomic force microscope tip using an electric field *Rev. Sci. Instrum.* **76** 046108